Enzymatically hydrolyzed fluorescence-based chemical probe enables in situ

1	Enzymatically hydrotyzed hubicsence-based enemical probe chables in suu
2	mapping of chitinase activity in the rhizosphere
3	Elias K. Zegeye ^{a,b} , Vivian S. Lin ^a , Jamie R. Nunez ^a , Nick A. Sconzo ^c , Samuel O. Purvine ^c ,
4	Aaron T. Wright ^{a,b,d,e} , James J. Moran ^{c,f,g,h} *
5	
6	Affiliations:
7	^a Biological Sciences Division, Pacific Northwest National Laboratory, Richland, WA, USA
8 9	^b The Gene and Linda Voiland School of Chemical Engineering and Bioengineering, Washington State University, Pullman, WA, USA
10 11	^c Environmental Molecular Sciences Laboratory, Pacific Northwest National Laboratory, Richland, WA, USA
12	dDepartment of Biology, Baylor University, Waco, Texas, 76798, USA
13	^e Department of Chemistry and Biochemistry, Baylor University, Waco, Texas, 76798, USA
14	f Department of Integrative Biology, Michigan State University, East Lansing, MI 48824, USA
15	g Department of Plant, Soil and Microbial Science, Michigan State University, East Lansing, MI,
16	48824, USA
17	^h Department of Crop and Soil Sciences, Washington State University, Pullman, WA, USA
18	
19	* Correspondence:
20	James J. Moran, Michigan State University, 288 Farm Lane, Rm. 203, East Lansing, MI, 48824,
21	USA: moranja7@msu.edu
22 23	Keywords: Chitin, Chitinase, Rhizosphere, Spatial analysis, Fluorescence probe
24	Reywords. Childing Childhase, Rinzosphere, Spatial analysis, Fluorescence probe
25	Abstract
26	Chitin is an insoluble and ubiquitous soil biopolymer, estimated to be the second most abundant
	commission in the second mean designation of the second mean d
27	organic soil biopolymer on Earth. Despite its abundance, role as a source of C and N in soil, and
28	importance to ecosystem function, further research is required to elucidate key controls on chitin
29	breakdown under varying environmental conditions. Previous work highlights the important role
30	rhizosphere microbiomes and root exudates can play in chitin catabolism. To enable mapping of
31	chitinase activity within the highly heterogeneous and spatially organized rhizosphere, we

designed and synthesized an enzymatically activated fluorogenic substrate, chitotriose-

TokyoGreen (chitotriose-TG), by incorporating a fluorescein derivative (TG) onto the trimeric unit

32

of chitin. This non-fluorescent substrate is selectively hydrolyzed by chitinase to release TG and yield a fluorescence signal, which can be used to spatially image and measure chitinase activity in the rhizosphere. To demonstrate the application of this technique, we grew switchgrass (*Panicum virgatum*) in rhizoboxes amended with a horizontal layer supplemented with chitin. We extracted mobile proteins from the rhizobox using a nitrocellulose membrane blotting technique which offers non-destructive enzyme extraction while preserving the 2D spatial position of the enzymes. We then subjected these membranes to the synthesized chitotriose-TG stain to spatially visualize the distribution of chitinase activity within the rhizosphere. We observed increased chitinase activity near switchgrass roots and higher activity within the soil zone enriched in chitin, showing an adaptive response of chitinase production with spatial focusing in areas of higher chitin abundance. Thus, the enzyme extraction and visualization strategy we describe here can enhance efforts to better understand spatial controls on chitin breakdown in rhizosphere, further elucidating the role of chitin as a C and N source in these systems.

1. Introduction

The rhizosphere is the dynamic and complex plant-associated soil region frequently associated with elevated biogeochemical activity with relevance to many global nutrient cycles (Gobran et al., 1998; Kuzyakov and Razavi, 2019). The interface of plant roots, nutrients, soil, and microbes which constitute the rhizosphere represents a unique and important environmental niche that is chemically, biologically, and physically complex and highly dynamic (Moran and McGrath, 2021). The rhizosphere constitutes only a small portion of microsites in total soil, yet it is the primary location for hotspots of extracellularly secreted enzymes from both roots and the soil microbiome (Spohn and Kuzyakov, 2014; Lovell et al., 2021). Current methodologies and omics-based techniques are beginning to reveal fundamental biochemical interaction

mechanisms in the rhizosphere, but the spatial distribution of enzyme activities within the narrow spatial confines of the rhizosphere remain largely unknown (Spohn and Kuzyakov, 2014; Pathan et al., 2020). Focused, molecular-scale analyses of small molecules and proteins within the rhizosphere may help resolve unknown and/or unanticipated mechanistic controls of C and N cycling with implications at larger ecosystem scales (Egamberdieva et al., 2010). Further, spatially tracking enzymatic activity could expand our understanding of how extracellular enzymes are regulated to enhance nutrient bioavailability and delivery to plant roots.

Chitin, a ubiquitous and abundant biopolymer of *N*-acetylglucosamine produced in soils as a major component of fungal cell walls and insects, can provide a source of N for plants and both C and N for soil microbes (Hanzlíková et al., 1989). This macromolecule needs to be decomposed into smaller bioavailable forms by various extracellular enzymes to enable uptake by plants or microbes (Chen et al., 2019). The presence of chitin in the rhizosphere is known to stimulate secretion of chitinases by plant roots and soil microbes to catabolize chitin and acquire the resulting bioavailable nutrients (Olander and Vitousek, 2000). Additionally, chitinase can be released by plants as a defense mechanism to protect from microbial pathogens, which enhances plant health and productivity (Sharma et al., 2011; Veliz et al., 2017). Consistent with this, plants have been observed to increase their root density into spatially constrained areas of increased nutrient abundance (Fransen et al., 1998; Hodge, 2004) and, similarly, microbes strategically colonize nutrient hotspots and secrete enzymes to degrade macromolecules into smaller and more bio-accessible nutrients (Compant et al., 2010; Mendes et al., 2013; Spohn and Kuzyakov, 2014).

Regulation of chitinase gene expression can be triggered by nutrient availability where the abundance of chitinases can vary spatially and temporally in the rhizosphere (Spohn and

Kuzyakov, 2014; Debnath et al., 2020). Understanding the spatiotemporal distribution of enzyme activities in the rhizosphere will provide valuable insight into microbial and plant nutrient acquisition strategies and the triggers that induce a shift from one strategy to another, helping contribute to a deeper understanding of nutrient cycling mechanisms and associated turnover rates (Ma et al., 2018a; Ma et al., 2018b). Many studies have evaluated extracellular enzymes using either isolated soil microbes or extracting a homogenized sample from rhizosphere (Barillot et al., 2013). However, neither of these approaches can identify and trace the fine-scale spatiotemporal distribution of these enzymes and their activities (Wei et al., 2021). Additionally, there are proteomics and transcriptomic-based approaches that can be used to investigate isolated soil microbiomes and their potential enzymatic activity. However, these classic 'omics techniques focus on enzyme/protein abundance, and they do not measure actual activity or spatiotemporal distribution of this activity in the rhizosphere (Chelius and Triplett, 2001; Torsvik and Øvreås, 2002; Kirk et al., 2004). Overall, this paucity of knowledge on the spatial distribution of enzyme activity constrains our ability to understand biogeochemical processes in a plant-microbe-soil interaction region.

80

81

82

83

84

85

86

87

88

89

90

91

92

93

94

95

96

97

98

99

100

101

102

There are efforts to develop efficient and explicit methods to spatially measure enzymatic activities in rhizosphere. Soil zymography is a widely used technique to map the distribution of enzyme activity. Spohn and coworkers successfully mapped the spatial distribution of protease and amylase activities of lupine (*Lupinus polyphyllus*) grown in rhizoboxes (Spohn et al., 2013). More recently, Ma et al. used soil zymography to study phosphatase activities in maize and lupine rhizosphere in response to pH changes (Ma et al., 2021). Soil zymography typically uses a colorimetric- or fluorescence-based substrate and correlates the disappearance of the substrate or the generation of product with the functional role of the enzyme of interest, which serves as a

proxy measurement for enzymatic activity. To optimize the detection of enzyme activities in soil systems, a wide range of studies have been performed to identify dyes that can be conjugated with certain substrates for spatial characterization of specific enzyme activities. Currently, 4-methylumbelliferone (MUF) and 7-amino-4-methylcoumarin (AMC) are known dyes that have been integrated with various substrates and used in the soil zymography techniques (Razavi et al., 2019). These dyes have been successfully applied in complex soil systems. Some of the applications include studying the role of enzymes in multiple biogeochemical cycles (Razavi et al., 2019), the effect of root morphology on the spatial pattern of enzymes (Ma et al., 2018b), the impact of nutrients on the distribution of microbial hotspots (Heitkötter and Marschner, 2018), and the effect of nematodes on the enzymatic activity of cellobiohydrolase and phosphatase in the rhizosphere (Razavi et al., 2017).

Building upon this prior work, we synthesized and applied an activatable fluorescence-based probe for chitinase activity by modifying chitotriose with a fluorescein derivative moiety, (6-hydroxy-9-(4-methoxy-2-methylphenyl)-3H-xanthen-3-one) (Tokyo Green, TG), to generate a probe that becomes fluorescent upon hydrolysis by chitinase. We demonstrated our probe technique by performing spatial mapping of chitinase activity in a chitin-supplemented switchgrass rhizosphere. Switchgrass (*Panicum virgatum*) is an established bioenergy crop, and it is also used for soil protection for ecosystem sustainability (Lovell et al., 2021).

To enhance our ability to spatially map chitinase activity in the rhizosphere, we sought to explore alternative approaches that could augment the existing zymography technique. Although there are some similarities between the approaches that we have utilized and the conventional zymography technique, there are also specific methodological distinctions. Both the conventional zymography technique and our method employ non-destructive sampling from the rhizosphere

and utilize a fluorogenic or colorimetric substrate to conduct in situ mapping of enzymatic activities. However, our methodology involves utilizing a multi-stage imaging and analysis technique. Initially, a nitrocellulose membrane was applied to extract mobile proteins from the rhizosphere. Next, the membrane and adsorbed proteins were stained with chitotriose-TG. The enzymatic reaction hydrolyzes chitotriose-TG and liberates hydrophobic TG, which has a high molar extinction coefficient and fluorescence quantum yield (Kamiya et al., 2005). In the conventional zymography techniques, a membrane or gel needs to be saturated with the fluorogenic substrate, then incubated with the rhizosphere (Spohn, 2014; Ma et al., 2021). This method may introduce a relatively large amount of enzyme substrate and agarose gel to the rhizosphere. The incorporation of these materials within the rhizosphere is expected to create an unfavorable environment that could potentially interfere with any subsequent experiments conducted in the rhizosphere, such as temporal studies or metabolomics analyses. Following protein extraction from the rhizosphere, we stained the nitrocellulose membrane using a buffer solution containing chitotriose-TG at the micromolar range. In contrast, the conventional zymography technique involves putting a fluorogenic dye-saturated nitrocellulose membrane on the rhizosphere to conduct enzymatic activities, but it requires the use of extremely large amount (millimolar range) of fluorogenic substrate. Our method involves a washing step to remove excess fluorogenic substrate, soil particles, and debris that could interfere with the imaging process, therefore it requires a careful design and synthesis of a fluorogenic substrate that can undergo hydrolysis and generate a hydrophobic fluorogenic product that adheres to its original position on the nitrocellulose membrane. Overall, the choice to employ either technique will depend on the specific experimental conditions, considering pros and cons of each method.

126

127

128

129

130

131

132

133

134

135

136

137

138

139

140

141

142

143

144

145

146

We analyzed chitinase activity using our novel fluorescent substrate and compared the impact of a chitin amendment on the spatial distribution of chitinase. We observed increased chitinase activity within the vicinity of added chitin. This result helps define the contribution and influence of plant and nutrient availability on the spatial distribution of chitinase activity in the rhizosphere. Our approach highlights the spatially focused physiological plasticity in plant and microbial communities as they adapt to heterogeneously distributed chitin resources in soil, which brings a broader functional understanding of chitin catabolism in rhizosphere. Finally, to identify the type and source of the chitinase activity observed using chitotriose-TG, we performed global proteomics on the chitin supplemented rhizosphere region (Fig. 1). Overall, these approaches can be combined with metatranscriptomics knowledge to better understand how the environment regulates chitin catabolism in soil, with implications for plant-microbe-soil interactions, plant productivity, and C cycling linked to soil health and, ultimately, ecosystem sustainability.

2. Materials and methods

2.1 Synthesis of chitotriose-TG

We used commercially supplied chitin (Beantown Chemical, Hudson, NH) as a starting material to synthesize chitotriose-TG (**Scheme S1**). We depolymerized and acetylated chitin using sulfuric acid and acetic anhydride to generate a white peracetylated chitotriose solid (Zegeye et al., 2021). Subsequently, this intermediate was chlorinated at the anomeric position using HCl gas (Zegeye et al., 2021). The chlorinated sugar was coupled with the TG, and its final product was obtained by deprotecting the acetyl groups from the hydroxyl moieties using sodium methoxide in methanol.

2.2 Validation of chitotriose-TG

We validated chitotriose-TG probe reactivity with chitinase using a staged approach, starting with purified enzymes and progressing toward systems of increasing biological complexity. First, we compared the fluorescence intensity of TG and chitotriose-TG by spotting 1 μL of 0.01-1.00 μM TG or chitotriose-TG in modified universal buffer (MUB) on nitrocellulose membrane. The membranes were then dried for 1 h and imaged using a FluorchemQ imager, Alpha Innotech (Ex/Em Cy2/Cy2). Fluorescence intensity was compared between TG and chitotriose-TG at different concentrations. Subsequently, this verification experiment was extended to a commercially available chitinase cocktail (Sigma-Aldrich, St. Louis, MO) derived from *Trichoderma virideas*. Chitotriose-TG (5 μM) was incubated with varying concentrations of chitinase (0.1-100 μg/mL) secreted from *Trichoderma virideas* for 30 min. TG (1 μM) and MUB buffer were used as a positive and negative control for this experiment, respectively. 1 μL of solution from each treatment was spotted on nitrocellulose membrane, dried for 1 h, and imaged as described above.

An enzymatic dose-response experiment was also conducted to analyze the kinetics of the fluorescence signal generated by chitinase-mediated hydrolysis of chitotriose-TG. Chitotriose-TG (1 µM) was incubated with varying amounts of chitinase (0.1-5 µg/mL), and the kinetics of the reaction were measured for 1 h. Finally, these two validation experiments were repeated using a secretome from *Cellvibrio japonicus* grown on chitin to represent a more complex biological system. *C. japonicus* was cultured using chitin as a carbon source to induce chitinase expression. The culture supernatant, including chitinase, was then collected to validate chitotriose-TG. The growth, harvest, and proteome sample preparation of *C. japonicus* has been described previously (Zegeye et al., 2021).

2.3 Rhizosphere preparation and switchgrass growth

Native soil was collected at Kellogg Biological Station (longitude: latitude 42.394230, -85.373633) in Michigan, USA from the surface to 15 cm depth (see description of physical soil properties in Robertson et al., 1997 and soil elemental composition in Ilhardt et al., 2019). To remove large debris, rocks, and organic material, the soil was sieved (4 mm mesh) and temporarily stored at 4 °C until switchgrass growth experiments. Subsequently, this native soil was homogeneously mixed with sand (40-100 mesh, Acros Organics) at a ratio of 1:3, soil:sand, w/w.

Rhizoboxes 20.3 cm x 25.5 cm x 2.0 cm (width x height x thickness) were constructed from transparent polyethylene with a removable side panel. Each rhizobox was filled with 1 kg of homogeneously mixed soil and sand. First, the rhizoboxes were filled approximately halfway with the soil/sand mixture, and then 1 cm layer of soil/sand mixture combined with 2 % [w/w] chitin was added. Finally, the rhizoboxes were filled by the soil/sand mixture. In total, we prepared 12 rhizoboxes for three treatment groups, each with four biological replicates. We placed a horizontal layer supplemented with chitin in rhizoboxes both with and without switchgrass. In parallel, a negative control treatment (with four replicates) was set up that contained switchgrass but without supplemented chitin.

Following the method described by Lin and coworkers, we germinated switchgrass seeds (*Panicum virgatum* L. var. Cave-in-rock; Lin et al., 2020). Germinated switchgrass seedlings were transplanted into the rhizoboxes, and all rhizoboxes were positioned (including rhizoboxes without switchgrass) at 45° angle to direct root growth only into the front panel of the rhizoboxes (**Fig. S2**). All rhizoboxes were wrapped with aluminum foil to protect from the light and placed in a growth chamber (28 °C and 60% relative humidity; Conviron, Pembina, N. Dakota) which was adjusted to a cycle of 16 h day and 8 h night. All rhizoboxes were watered with deionized

water (40 mL) two times per week for 4 months. The height and number of leaves of the switchgrass were recorded once every two weeks.

2.4 Fluorescence imaging

216

217

218

219

220

221

222

223

224

225

226

227

228

229

230

231

232

233

234

235

236

237

238

Modified universal buffer (MUB) stock was prepared by mixing Tris base (12.1 g), maleic acid (11.6 g), citric acid (14.0 g), boric acid (6.3 g), and 1 M NaOH (488 mL) and was brought up to 1 L by Milli-Q water. To make the working stock of MUB, 200 mL of MUB stock was used and its final pH was adjusted to 6.5 using HCl (1 M) or NaOH (1 M) and its volume was adjusted to 1 L using Milli-Q water. Nitrocellulose membrane (Bio-Rad, Hercules, CA, 100% nitrocellulose, 0.45 µm pore size) were cut to cover the sampling area (15.5 cm x 8.5 cm, width x height) of the rhizoboxes. To spatially measure chitinase activity, first, the rhizoboxes were carefully opened by removing the front panel without physically disturbing the rhizosphere soil (Fig. S4). Subsequently, a nitrocellulose membrane was positioned in the sampling area of the rhizobox and a thick filter paper placed on top of the membrane to increase the contact surface area between the rhizosphere and membrane, which enhance the protein transfer through diffusion from the wet surface of the rhizosphere to the dry area of membrane. The front panel was replaced and the rhizoboxes returned to the growth chamber and incubated for 24 h. On the following day, all the rhizoboxes were again carefully opened and the membranes were collected with tweezers to immediately stain using MUB buffer containing chitotriose-TG (2 µM) for 30 min with agitation. Chitotriose TG-stained membranes were washed with SYPRO wash (10% methanol and 7% acetic acid in deionized water) for 24 h to remove excess fluorescent dye. The next day, the washed membranes were air-dried and imaged using a FluorchemQ (Alpha Innotech, CA,

USA) instrument with Ex/Em Cy2/Cy2 (Fig. S4).

2.5 Fluorescence image analysis

The fluorescence signal generated on the membrane was measured and analyzed to compare chitinase activity under different biological conditions using a custom Python (v 3.9.7) code. To develop and construct the image analysis code, we utilized the following packages: OpenCV (v 4.5.3), matplotlib (v 3.5.0) (Hunter, 2007), numpy (v 1.20.3) (Van Der Walt et al., 2011), and seaborn (v 0.11.2) (Waskom et al., 2018), scipy (v 1.7.3) (Virtanen et al., 2020), and pandas (v 1.3.5) (Reback et al., 2020). Additionally, we used an interactive Python environment, Jupyter Notebook (v 6.4.6), to develop tabulated figures and interpretable data. All code is provided at github.com/pnnl/exima.

To differentiate between root and soil regions, masks were manually drawn onto the image of the rhizobox based on visual identification of the boundaries between root edge and adjacent soil. Root that was not visible (e.g., beneath the surface) was not included in the mask. The same was done to annotate the supplemented nutrient location. Pixel locations of the rhizobox and membrane boundaries were used to align the rhizobox image (i.e., root mask) to the membrane image, ultimately providing root location alongside signal from the membrane stain. Images were then cropped to remove membrane edges (which contain artifacts resulting from membrane handling). Image data was normalized to ensure soil above the nutrient band far from the root (25+ pixels away from the nearest root pixel) had an average of 0 and standard deviation of 1. The normalized fluorescence signal (AU, arbitrary unit) is used to compare the chitinase activity across treatments and replicates. Further details and an example notebook are stored on the above GitHub repository link.

2.6 Metaproteomics

After 4 months of switchgrass growth, \sim 10 g of soil/sand was collected from each rhizosphere (12 rhizoboxes) from within the nutrient localized horizon. The harvested soil was immediately stored at -80 °C in a 50 mL Falcon tube. We used the protein extraction and subsequent proteomics analysis methods described by Nakayasu et al. (2016) and Steinke et al. (2020). We carried out the proteomics experiment using all 12 samples. For protein extraction, soil samples (10 g) were mixed with 10 mL of a mixture of stainless-steel, garnet, and silica beads. Then, we added 20 mL ice-cold chloroform:methanol (2:1, v/v) and 4 mL cold ultrapure water to the soil and beads mixture. Samples were vortexed horizontally (10 min, 4 °C) and probe sonicated (60% amplitude, 30 sec) using a FisherBrand model number FB505 sonicator (500 W, 20 kHz) that was integrated with Fisherbrand replaceable probes with a model number FB4420. Following sonication, we centrifuged (4,000 x g, 5 min, 4 °C) and separated the protein and soil pellets. Both pellets were dried using the turbo vacuum drier, flash frozen, and stored in a -80 °C freezer for the subsequent steps.

We prepared 200 mL protein solubilization buffer by mixing 8 g sodium dodecyl sulfate (SDS), 3.08 g dithiothreitol (DTT) and 10 mL 1 M Tris and Milli-Q water. Then, we added this solubilization buffer to the protein pellets (10 mL) and soil pellets (20 mL), and samples were sonicated (20% amplitude, 30 sec) with the same sonicator described previously. To ensure the protein was properly solubilized with the buffer, we placed each sample into a tube rotator (30 min, 300 rpm, 50 °C) and horizontally vortexed to evenly mix and solubilize proteins. Samples were centrifuged (4,000 x g, 5 min, room temperature) and supernatants were collected from protein and soil pellets; the supernatants were then combined into a new 50 mL Falcon tube. To further extract the remaining proteins, we added 100 mM (NH₄)HCO₃ into the soil (20 mL) and

protein pellets (10 mL). In a similar way, we sonicated (20% amplitude, 30 sec), centrifuged (4,000 x g, 5 min, room temperature), and then collected the supernatants. The extracted proteins were precipitated using 20% trichloroacetic acid (TCA), 7.5 mL TCA used for the 30 mL supernatant. To enhance protein precipitation, we placed samples in a -20 °C freezer overnight. The next day, samples were centrifuged (4,000 x g, 10 min, 4 °C), and the protein pellets were collected. We washed the protein pellets using 100% ice-cold acetone (2 mL) three times. During each wash, samples were centrifuged (4,000 x g, 10 min, 4 °C) and supernatants were decanted into waste. Finally, the washed protein pellets were dried under nitrogen and resuspended again using 200 μ L protein solubilization buffer. To completely dissolve the resuspended proteins, samples were sonicated and heated (90 °C, 5 min). Following heating, samples were centrifuged (4,500 x g, 10 min, 4 °C) and supernatants were stored in a -80 °C freezer.

To prepare samples for protein digestion, we performed filter-aided sample preparation (FASP). A solution of 8 M urea in 50 mM (NH₄)HCO₃ (400 μ L) and the supernatant from the previous steps were added and mixed into a filter column. Samples were centrifuged (14,000 x g, 30 min) and the flow-through was discarded. Then, we rinsed samples three times with 400 μ L urea solution. Additionally, we washed samples four times with 50 mM ammonium bicarbonate (100 μ L). Following the washing step, we added 50 mM (NH₄)HCO₃ (75 μ L) and trypsin digestion buffer (4 μ L) to the column after placing the column in a 1.5 mL FASP tube. Samples were incubated (37 °C, 750 rpm, 3 h) and additional 50 mM (NH₄)HCO₃ (40 μ L) was added. Then, samples were centrifuged (14,000 x g, 15 min) and we collected peptides and dried them using a speed vacuum. Finally, we resuspended peptides with 5% acetonitrile (30 μ L) and stored them in a -80 °C freezer until analysis.

The bottom-up proteomics methodology we used was described in detail by Steinke et al. (2020). Additionally, we used customized reverse-phase capillary HPLC columns coupled with a tandem mass spectrometry (LC-MS/MS) as described by Slysz et al. (2014). Briefly, the capillary LC columns were prepared by packing a slurry of 3 µm Jupiter C18 stationary phase (Phenomenex, Torrance, CA) into a 60 cm long fused silica capillary tubing (Polymicro Technologies Inc., Phoenix, AZ) with an outer diameter of 360 µm and an inner diameter of 75 um, which was fitted with a 1 cm sol-gel frit to retain the packing material. Peptide samples were subjected to capillary liquid chromatography and analyzed by LTQ Orbitrap Velos mass spectrometer (Thermo Fisher). Formic acid (0.1%) in water and formic acid (0.1%) in acetonitrile were used as a mobile phases (Slysz et al., 2014). The raw spectra collected from LC-MS/MS converted to mzML using MSConvert (Kim and Pevzner, 2014). Each LC-MS/MS data file was searched against 21 genomes and metagenomes (for list, see supplemental materials). In cases of very large search files (i.e., files 2 through 8 as listed in the supplemental materials) we used a 15 part splitting of the fasta files to accommodate memory usage limitations, and these files were searched only using Tryptic cleavage rules, +/-20 ppm parent mass tolerance, and no post-translational amino acid modifications. All other files used partial tryptic cleavage rules, +/-20 ppm parent mass tolerance, and allowed the possibility of oxidized methionine. Results were collated and each genome filtered using a target/decoy approach and adjusting the MSGFPlus Q-Value to ~1% False Discovery Rate (Elias and Gygi, 2007). The highest MSGFScore scoring peptide from the 21 searches per MS/MS scan was retained as being the best peptide to spectrum match (PSM). MS/MS precursor mass signals were extracted from LC-MS/MS files using MASIC and StatMomentsArea values used for label free quantitative data. MS/MS spectra were counted per peptide to provide spectral count data. Peptides were

305

306

307

308

309

310

311

312

313

314

315

316

317

318

319

320

321

322

323

324

325

326

assigned to the first protein in which they were observed in the protein search file, so-called "first hits" protein inference approach. Peptides were grouped by their respective assigned protein and a crosstab of protein information derived from the peptide spectral counts and/or MASIC abundance values was developed. The protein crosstab included functional annotations such as EC, KO, product names and taxonomy.

3. Results

328

329

330

331

332

333

334

335

336

337

338

339

340

341

342

343

344

345

346

347

348

349

3.1 The fluorescence signal of chitotriose-TG when activated by chitinase enzymes

We first validated that chitotriose-TG is a useful indicator of chitinase activity by comparing the fluorescence signal between the TG and chitotriose-TG (Fig. 2A) in the absence of biological material. TG produced strong fluorescence signal while the chitotriose-TG appeared almost non-fluorescent (Fig. 2B). This preliminary experiment demonstrated that the chitotriose-TG itself does not generate intense fluorescence signal. Subsequently, we confirmed chitotriose-TG is activated by chitinases by incubating a pure chitinase cocktail secreted from Trichoderma virideas with chitotriose-TG (Fig. 2B and C). To investigate the correlation between fluorescence intensity generated from chitotriose-TG and chitinase activity, we conducted a chitinase dose response experiment on a nitrocellulose membrane (0.1-100 µg/mL chitinase) and a microplate reader (0.1-5 µg/mL chitinase) with chitotriose-TG. Both results from the membrane (Fig. 2B) and microplate reader (Fig. 2C and Fig. S1) showed that increasing enzyme concentration leads to increased fluorescence intensity. In these validation experiments, the TG was used as a positive control which correlated to the highest fluorescence signal, and no appreciable increase in fluorescence was observed for samples incubated without enzymes.

The chitotriose-TG was further validated using a relatively more complex proteome sample derived from a chitin grown *C. japonicus* secretome. This proteome sample contains a well-characterized chitinase (Zegeye et al., 2021), which is useful for evaluating the enzymetriggered hydrolysis of the chitotriose-TG. Similarly, we conducted an enzyme dose response experiment on a nitrocellulose membrane (**Fig. 3A**) and a fluorescence microplate reader (**Fig. 3B**). Both experiments showed a positive correlation between enzyme concentration and fluorescence intensity. These results indicate that the chitotriose-TG can be triggered by active chitinase to liberate the fluorescent TG to quantify chitinase-specific activity.

3.2 Impacts of chitin amendment on switchgrass growth

Switchgrass height and number of leaves were recorded every two weeks (**Fig. 4**). All switchgrass increased in height linearly until week 7 and stabilized during the remaining growth period. Switchgrass grown in rhizoboxes with supplemental chitin grew taller (p-value=0.038, week 14th time point) and had a higher number of leaves (p-value=0.032, week 14th time point) than switchgrass without chitin. The dry biomass weight of switchgrass grown with and without chitin was compared (**Fig. S3**). The switchgrass that had been grown with chitin exhibited a greater dry biomass than those that had been grown without the chitin supplement (p-value=0.0003).

3.3 Chitin availability in the rhizosphere increases chitinase activity

We used the chitotriose-TG probe to evaluate and compare chitinase activity related to chitin availability in the rhizosphere. The averaged quantified fluorescence signal linked to chitinase activity was compared among rhizosphere that were treated with switchgrass only (no chitin amendment control), chitin only (no plant control), or switchgrass and chitin amendment

together (**Fig. 5**). We found higher average fluorescence signal intensity correlating to increased chitinase activity in treatments with chitin amendments versus the switchgrass only treatments. The fluorescence signal for the soil and roots region were assessed separately and both results are nearly similar (**Fig. 5**). Further, rhizoboxes containing switchgrass without supplemental chitin showed an overall lower chitinase activity compared to their chitin amended counterparts. The quantified and normalized average fluorescence signal intensities were statistically compared; samples incubated only with chitin were significantly higher (p-value =0.03) compared to rhizosphere that was incubated with switchgrass and no chitin (**Fig. 5**). On the other hand, the average value of fluorescence signal observed from samples containing both chitin and switchgrass showed higher chitinase activity compared to the average value of switchgrass incubated without supplemented chitin, but this was not statistically significant (p-value on root=0.31, p-value on soil=0.30) (**Fig. 5**).

At an increasing spatial scale, we also used the chitinase activity assay to quantify differences within the amendment horizon itself as well as in the rhizobox soil layers above and below the zone of chitin supplementation. The average fluorescence signals across the biological replicates were measured and plotted using a two-dimensional histogram to indicate chitinase activity distribution in the rhizosphere (**Fig. 6**). Overall, the top layer of the rhizobox exhibited lower chitinase activity, while the chitin supplemented region and the lower section of the rhizosphere both displayed higher chitinase activity. We hypothesize that some of the chitin and/or chitinase might diffuse downward over the four months incubation time. The general trend of this result is observed in both soil and root areas.

3.4 Protein identified in the rhizosphere

The rhizosphere proteomics data were analyzed to identify chitinase and other glycosyl hydrolase (GH) enzymes. The number of proteins obtained from different rhizosphere treatments are tabulated in **Table 1**. In total, 25 chitinases, 117 other non-chitinase GH enzymes, and 81,715 proteins were identified. From the total number of chitinases identified in all treatments, the majority of chitinase (64.4%) enzymes were identified in samples collected from the switchgrass plus chitin rhizoboxes. Of the total number of chitinase identified, 13 were of microbial origin and the remaining 12 were linked to switchgrass. We observed that *Actinobacteria* and *Actinomycetales* are the major microbial chitinase contributors. Of the identified non-chitinase GH enzymes, 84.6% were of microbial origin and the remaining 15.4% were associated with switchgrass. We note that proteins linked to switchgrass were observed in the switchgrass-free rhizobox controls and attribute these features to relic proteins (or peptides) present in the soil prior to harvest, since this soil has been in constant switchgrass production for over a decade, since 2008 (Robertson and Hamilton, 2015). This would be consistent with the reduced number of proteins observed in these control samples.

4. Discussion

To gain insights into how enzymes regulate biogeochemical processes, it is crucial to have the ability to track spatiotemporal enzymatic activity in the rhizosphere (Liu et al., 2017). The fundamentally small scale of the rhizosphere combined with the inherent heterogeneity of plant root exudation and resulting microbial activity make this a very complex system (Nuccio et al., 2020). The high rates of microbial processes can have substantial impact on local biogeochemistry that influence processes at the plant or larger scales. Here, we studied chitin

catabolism in rhizosphere given its abundance in nature and key role in both C and N cycling in ecological food webs (Brzezinska et al., 2014). Rhizosphere microbiomes and root exudates are principal drivers of chitin degradation and the associated release of C and N which impacts plant health and overall soil fertility (Whipps, 2001; Beier and Bertilsson, 2013). Thus, a robust approach to elucidate the spatial distribution of chitinase in rhizosphere will ultimately help determine key functional drivers of chitinolytic process and their phenotype response in environmental change.

The diverse sources of chitinase along with the biological and physicochemical complexity of rhizosphere complicate effective tracking of chitinase in rhizosphere (Neiendam Nielsen and Sørensen, 1999; Nisa et al., 2010). To overcome challenges associated with studying chitinase activity in soil, we developed a fluorogenic chitinase substrate (chitotriose-TG) that enables spatially resolved, minimally destructive measurement of chitinase activity along roots, and in soil of rhizoboxes.

The fluorescent probe we designed, chitotriose-TG, contains a trimeric unit of chitin that allows and guides the probe to selectively react with chitinases. In its intact form, this probe is non-fluorescent (**Fig. 2B**), but upon reaction with chitinase, the probe is cleaved, and a fluorescence signal is produced (**Fig. 2 and 3**). Additionally, this enzymatic hydrolysis converts the hydrophilic substrate (chitotriose-TG) into a hydrophobic fluorescence product (TG) which limits its diffusion away from its initial position (Kamiya et al., 2005); therefore the spatial distribution of the fluorescence signal reflects the initial active chitinase location. Kamiya et al. (2005) blotted TG on a nitrocellulose membrane and examined its hydrophobicity by subsequent washing and similarly reported that the TG retained its original spatial position (Kamiya et al., 2005). This particular property of the chitotriose-TG provides a useful advantage for analyzing

the spatial distribution of enzymes that were extracted by membrane blotting from the rhizosphere.

Plant interactions with soil include a range of bio- and geo-chemical processes, including a variety of enzymatic interactions and their associated regulation (Génard et al., 2014). We used rhizoboxes containing different chitin amendments to explore various growth dynamics of switchgrass to gain insight about spatial controls of chitinase activity. The chitin supplemented switchgrass grew taller, had a higher numbers of leaves, and showed increased dry biomass compared to the non-chitin supplemented switchgrass, demonstrating the presumed link between chitin amendment and increased plant nutrient acquisition (**Fig. 4 and Fig. S3**). This result is consistent with prior research that reported chitin as a biostimulator and a nutrient source for plant growth (Li et al., 2020). Catabolized chitin likely triggers signaling to enhance plant photosynthesis and C and N metabolism, which contributes to boost growth (Winkler et al., 2017; Zhang et al., 2018). Presumably these impacts are only made possible through breakdown of chitin by various chitinases and associated enzymes. Thus, the observed higher growth of switchgrass in the chitin supplemented rhizoboxes is likely linked to subsurface chitinase activity.

Using our fluorogenic chitinase substrate, we measured and elucidated the distribution of chitinase activity in response to background or elevated chitin availability within the rhizoboxes. The overall number of identified chitinases (**Table 1**) and their activities (**Fig. 5**) were higher in the chitin-supplemented rhizosphere, and we observed higher chitinase activity spatially distributed along the chitin localized areas and further down in the rhizosphere (**Fig. 6**). These results represent an adaptive response to improve nutrient return from the added resource (i.e., chitin) through both switchgrass and microbial responses. Enzymatic activity within the

rhizosphere is dynamic and spatially varied, thus understanding how the heterogeneous distribution of chitin in soil regulates chitinase secretion provides insight about overall controls on chitin breakdown. The exact processes for upregulation of these chitinases is unknown, but we observed both switchgrass and microbially associated chitinases in chitin amended areas, likely representing an attempt at improving the nutrient conditions for growth. Additionally, the soil/sand mixture we used is nutrient limited, especially after 4 months of growth, the observed enzymatic response is likely related to nutrient acquisition or mobilization of nutrients from chitin due to nutrient limitation. Thus, the higher chitinase activity in the vicinity of chitin appeared because both microbes and switchgrass likely invested their chitinase production on a strategic beneficial area. In our proteomics data analysis, we identified chitinase and other nonchitinase GH enzymes (Table 1). Chitin catabolism requires the activity of multiple chitinase and associated GH enzymes (Beier and Bertilsson, 2013). In addition to chitinase, these GH enzymes might activate chitotriose-TG by hydrolyzing the glycosidic bonds at the anomeric position through promiscuous enzymatic activity. Notably, the chitinase activity patterns we observed using chitotriose-TG (Fig. 5) may not fully reflect the type or abundance of proteins that identified by the proteomics data (**Table 1**) as our approach is only sensitive to active enzymatic activity and not to inactivated or partially degraded enzymes. The chitotriose-TG specifically measures the function of chitinases or other non-chitinase GH enzymes involved in chitin catabolism based on their activity, while mass spectrometry reports on total proteins or peptides observed in the sample, regardless of active or inactive state. Future efforts could extend this approach by using chitotriose-TG to spatially identify hotspots of chitinase activity and then selecting that specific region of the sample for spatially resolved proteomic analysis (White et al., 2021).

461

462

463

464

465

466

467

468

469

470

471

472

473

474

475

476

477

478

479

480

481

482

Overall, we extended our previous methodology (Lin et al., 2020), and measured chitinase activity spatially on rhizosphere. Our approach involves protein extraction using a membrane from the rhizosphere, followed by fluorogenic staining and washing steps. In the future, further research is necessary to evaluate the extent of the nitrocellulose membrane's effectiveness in extracting proteins from the rhizosphere. Additionally, detailed experimental comparison of our approach with the conventional zymography is required in future investigations.

5. Conclusion

Overall, we developed and applied a strategy to spatially measure chitinase activity in soil systems with sufficient spatial resolution for interrogating the rhizosphere. We used this approach to identify increased chitinase activity in soil amended with chitin, which also improved switchgrass growth. In the future, this application can be integrated with omics techniques to fully analyze the spatiotemporal dynamics of chitinase activity in the rhizosphere. Understanding controls on chitinase activity and environmental drivers of activity is a central component toward better understanding and predicting overall C and N biogeochemistry of these dynamic systems.

6. Acknowledgements

The authors acknowledge Nathan Johnson for his efforts in helping develop and refine Figure 1. This work was funded by the DOE Office of Science Early Career Research Program Award (PI, JJ Moran). Battelle operates PNNL for the DOE under contract DE-AC05-7601830. A portion of this research was performed using EMSL (Project 51648), a DOE Office of Science User Facility sponsored by the Biological and Environmental Research program. Support for this research was also provided by the NSF Long-term Ecological Research Program (DEB 1832042)

at the Kellogg Biological Station and by Michigan State University AgBioResearch. We thank the USDA-ARS National Plant Germplasm System (NPGS; https://www.ars-grin.gov/Pages/Collections) for providing switchgrass seeds.

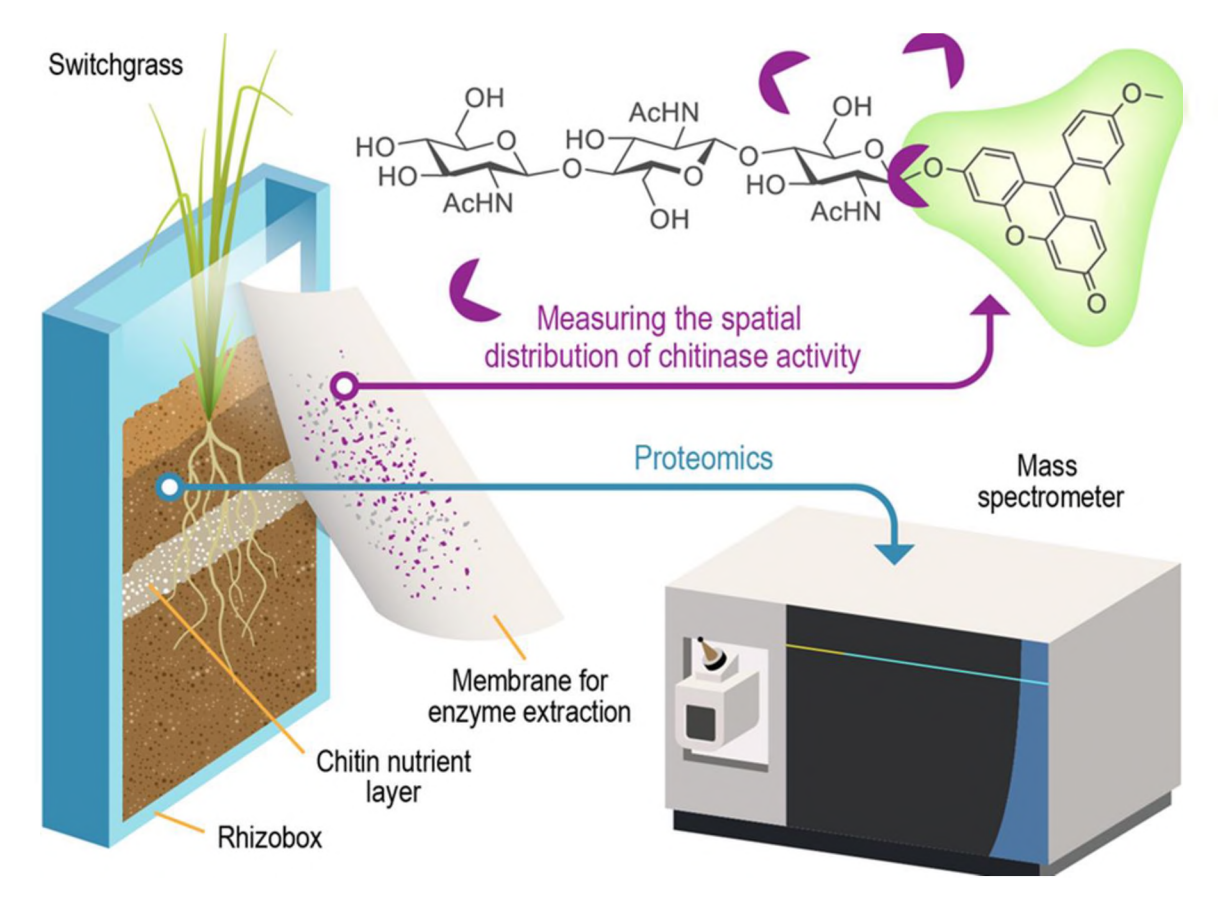
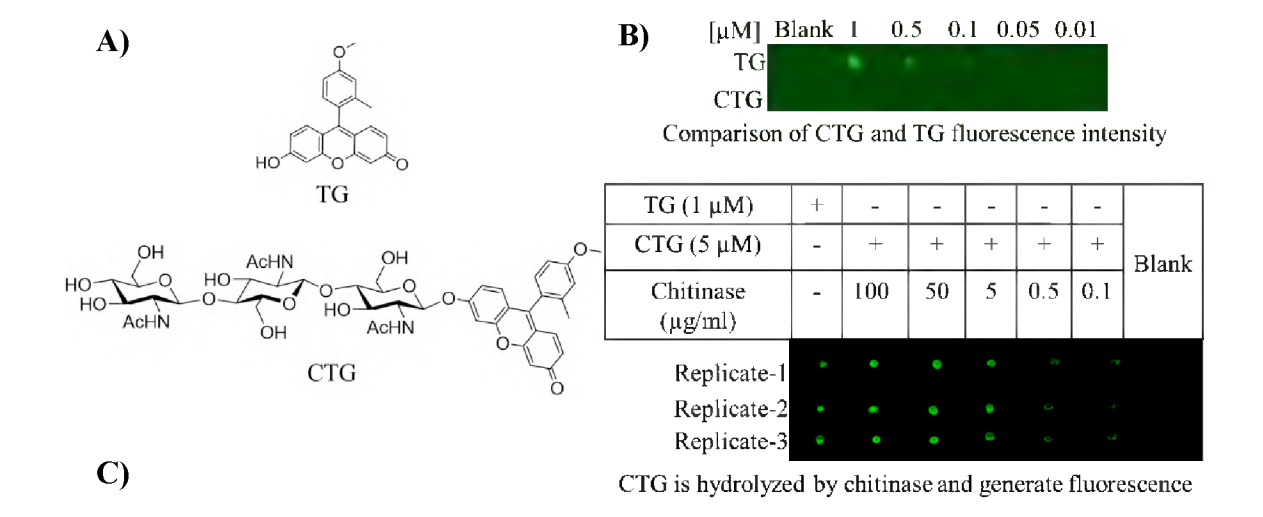


Fig. 1. The general strategy to spatially analyze chitinase activity in rhizosphere systems. Nitrocellulose membrane is used to extract proteins from the rhizosphere without disturbing the soil in the rhizobox. Subsequently, the membrane is stained with chitotriose-TG followed by imaging to visualize the fluorescent product, which can reveal the distribution of chitinase activity. Finally, samples were collected for a proteomics experiment aimed at identifying the type and source of chitin catabolizing enzymes in the rhizosphere.



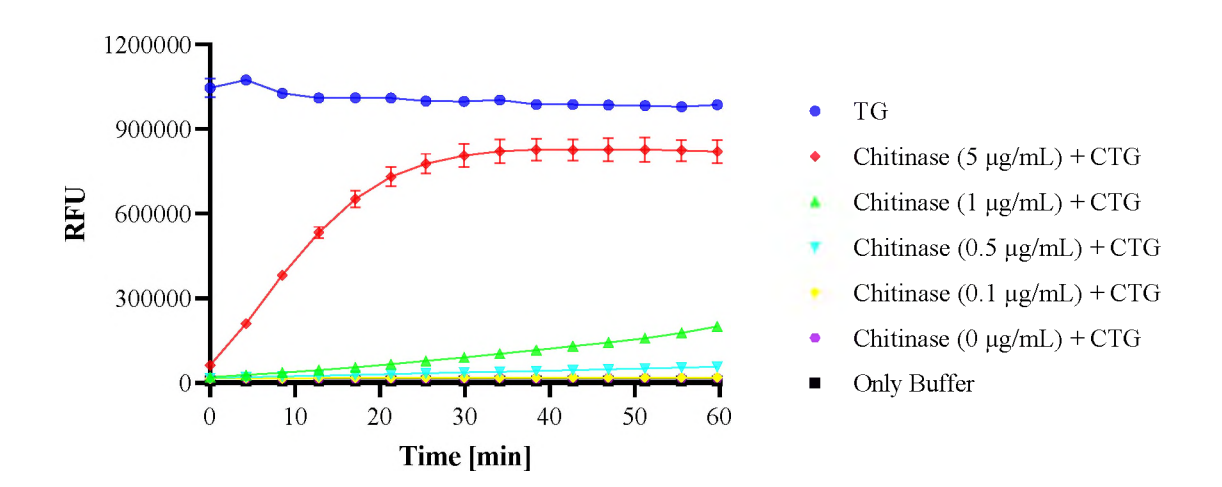


Fig. 2. Validation of chitotriose-TG using nitrocellulose membrane and fluorescence microplate reader. A) The chemical structure of TokyoGreen (TG) and chitotriose-TG (CTG). B) The fluorescence intensity of TG and chitotriose-TG were compared on a nitrocellulose membrane. A comparison was made by blotting 1 μ L of TG or Chitotriose-TG in MUB on nitrocellulose membrane in the absence of any enzymes (top membrane). Chitinase concentration ranging from 0.1 to 100 μ g/mL were incubated (30 min) with chitotriose-TG (5 μ M). 1 μ L from each set of reactions was placed onto the membrane with three technical replicates (bottom membrane). C) Kinetic measurements of the reaction between various chitinase concentrations (0.1-5 μ g/mL) and chitotriose-TG (1 μ M) were performed. The relative fluorescence units (RFU) of these reactions were recorded and plotted against for the 1 h duration. Chitinases were obtained from *Trichoderma virideas*. In both panel B and C, the enzyme free buffer and the TG were used as negative and positive controls, respectively.

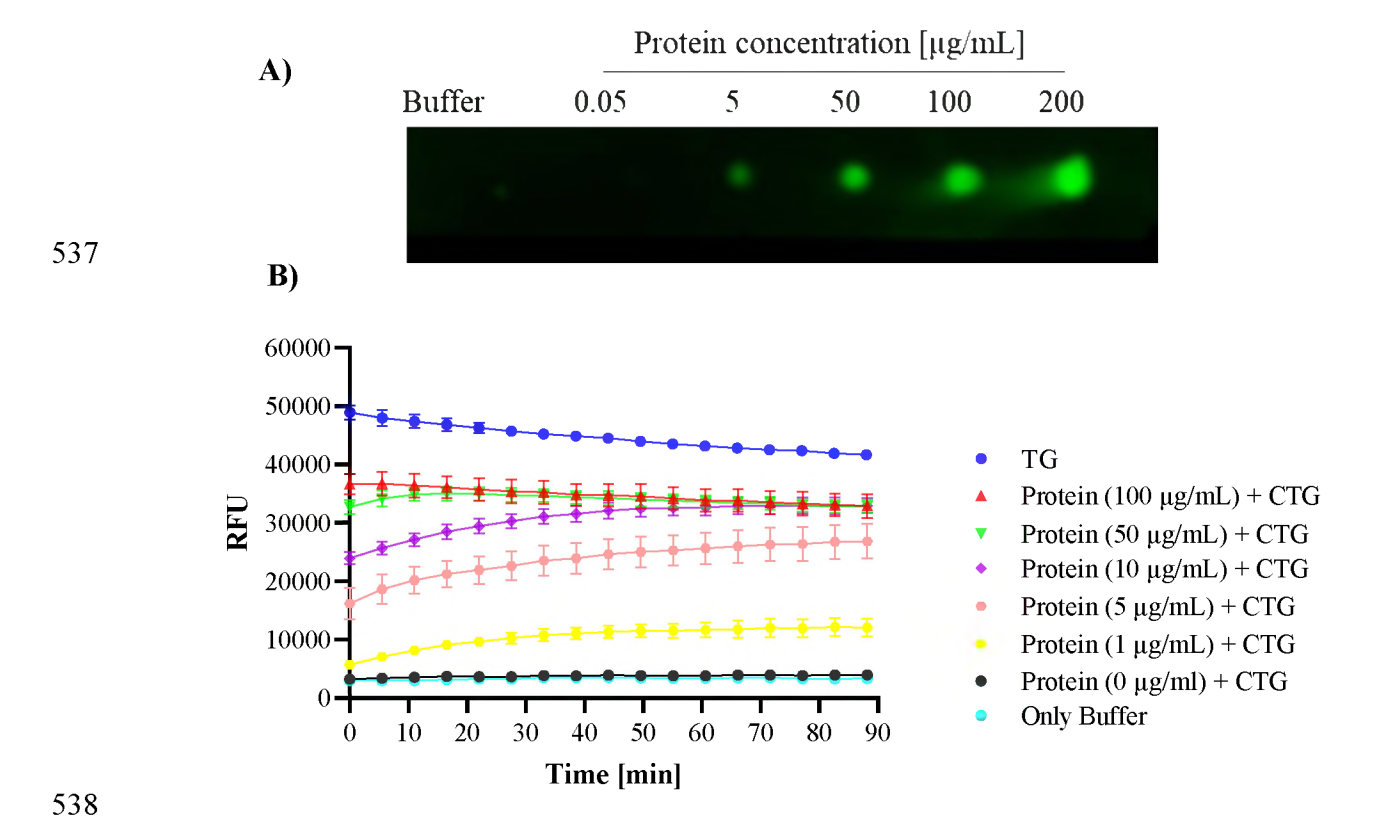
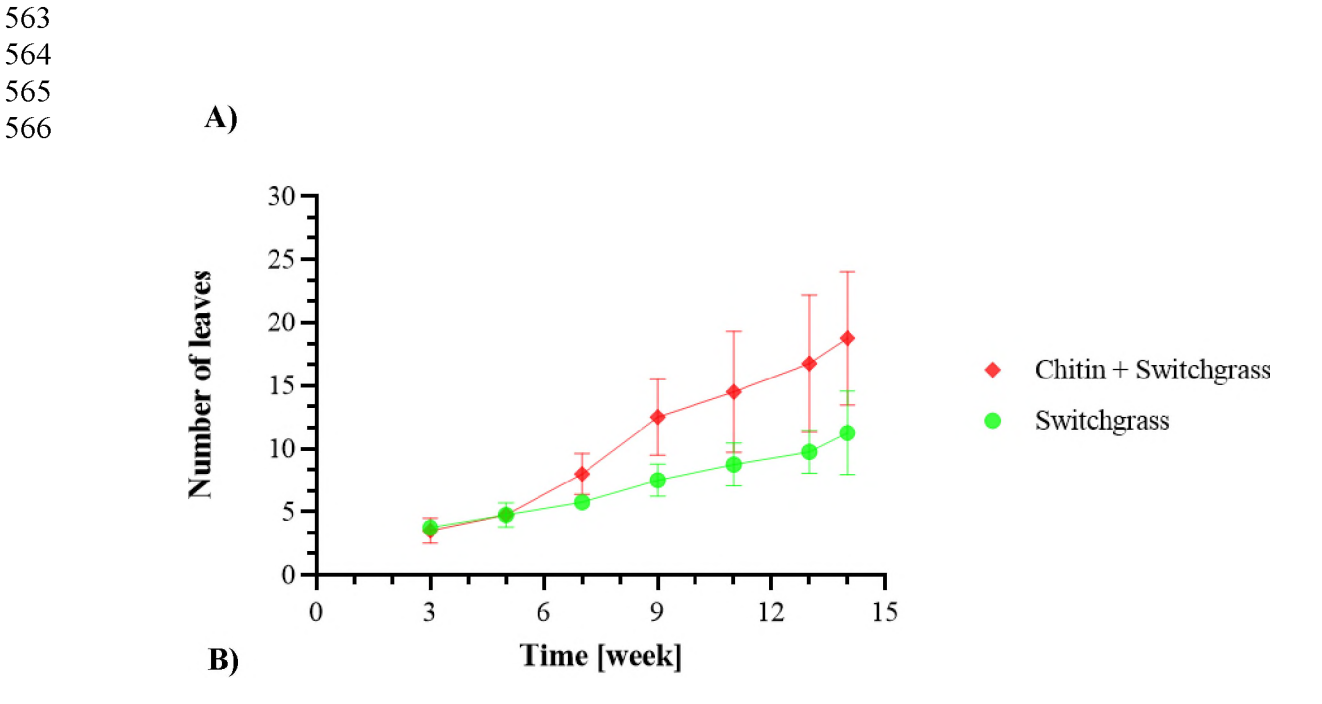


Fig. 3. Validating response of chitotriose-TG toward chitinase activity using a chitin grown *C. japonicus* secretome. A) A range of protein concentrations (0.05-200 μg/mL) were incubated with chitotriose-TG (5 μM) for 30 min and blotted (1 μL) on a nitrocellulose membrane. B) The proteome sample at various protein concentrations (1-100 μg/mL) were incubated with chitotriose-TG (5 μM). The relative fluorescence unit (RFU) were measured for 1.5 h on a microplate reader. The enzyme-free buffer and TG are used as negative and positive controls, respectively. TG=TokyoGreen, CTG= chitotriose-TG



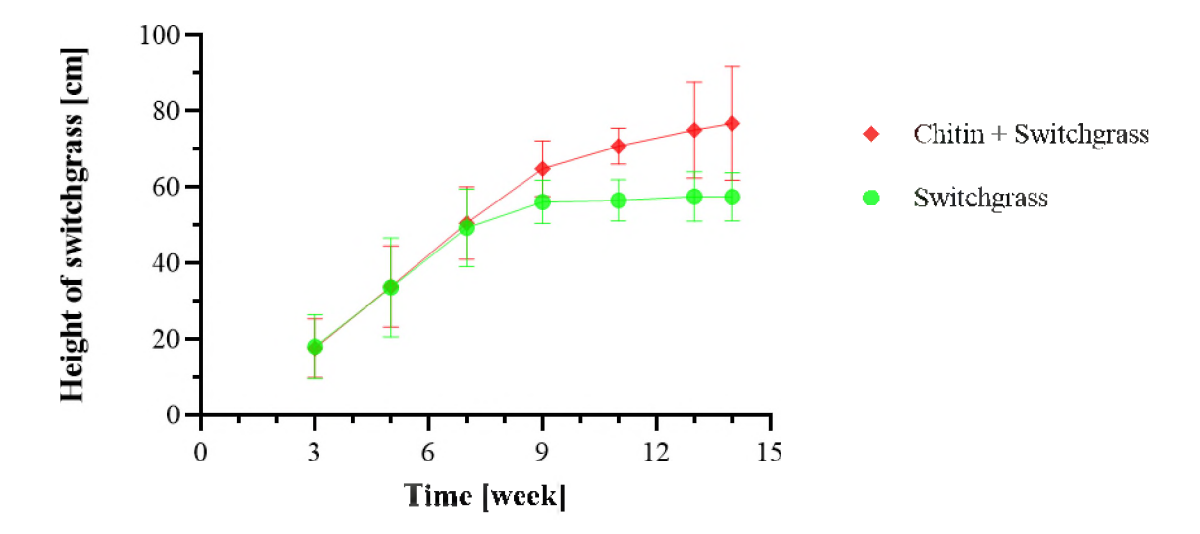


Fig. 4. The growth rate of switchgrass was evaluated under two conditions, with and without chitin availability, n=4. The height and number of leaves of each switchgrass was documented every two weeks. The average number of leaves (A) and height (B) of the switchgrass plotted per their growth time. The error bars represent the standard deviation of each condition.



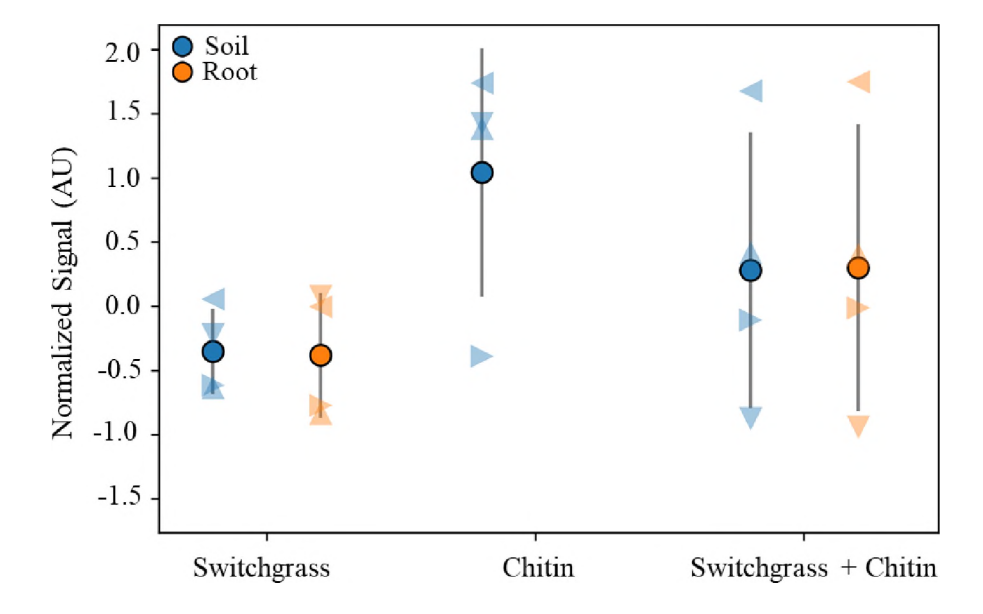


Fig. 5. Chitinase activity measurement on the rhizosphere. Proteins were extracted using a nitrocellulose membrane from three different treatments that consists of switchgrass, chitin, or switchgrass and chitin. Nitrocellulose membranes were stained with chitotriose-TG and the fluorescence signal quantified as a proxy for chitinase activity. The fluorescence signal from the nutrient amended horizon region was normalized using the top region of the rhizosphere. The normalized fluorescence signal of each replicate and its average value were plotted for each treatment. The standard deviation of the normalized average fluorescence signal is indicated by the gray line. The fluorescence signal from soil (blue) and switchgrass roots (orange) are shown separately. Each treatment consisted of four biological replicates, replicate 1= ▲, replicate 2=▶, replicate 3=▼, replicate 4=◄, average value of each treatment = ●.

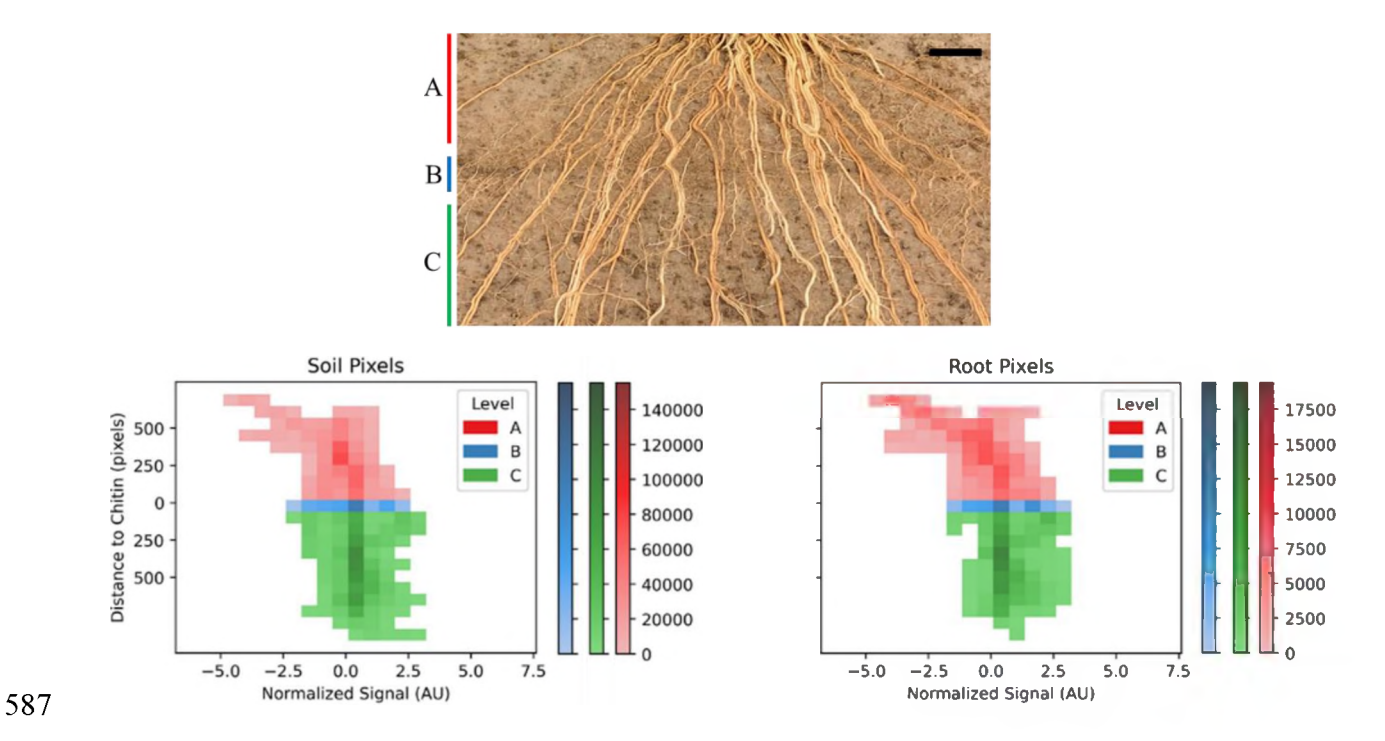


Fig. 6. The spatial distribution of root image and chitinase activity on rhizoboxes containing both switchgrass and chitin. The rhizosphere image displays the specific area that is used for the analysis of the chitinase activity (top). The normalized average fluorescence signal generated by the soil (bottom, left) and the switchgrass roots (bottom, right) indicates the spatial distribution of chitinase activity. Plot showing the normalized average fluorescence signal as a function of the distance from the added chitin. A= above the chitin, B= the supplemented chitin region, and C=below chitin. Scale bar = 15 mm

Table.1. Unique proteins counted from proteomics analysis.

Treatment	Replicate	Chitinase		Glycosyl hydrolase		All proteins	
groups		Switchgrass	Microbial	Switchgrass	Microbial	Switchgrass	Microbial
	1	0	0	0	6	86	5149
	2	5	0	10	31	702	30144
Switchgrass	3	1	0	2	22	212	19646
	4	0	0	5	14	210	10495
	Total	6	0	17	73	1210	65434
	1	0	0	0	4	71	3899
	2	0	9	0	4	89	8755
Chitin	3	0	0	0	4	51	3216
	4	0	0	0	5	44	3289
	Total	0	9	0	17	255	19159
	1	2	0	4	5	358	4918
Switchgrass	2	6	2	11	9	738	10825
+	3	2	3	4	3	132	4014
Chitin	4	4	1	3	3	228	3158
	Total	14	6	22	20	1456	22915

7. References

- Barillot, C.D., Sarde, C.-O., Bert, V., Tarnaud, E., Cochet, N., 2013. A standardized method for
- the sampling of rhizosphere and rhizoplan soil bacteria associated to a herbaceous root system.
- Annals of microbiology 63, 471-476.
- Beier, S., Bertilsson, S., 2013. Bacterial chitin degradation—mechanisms and ecophysiological
- strategies. Frontiers in microbiology 4, 149.
- Brzezinska, M.S., Jankiewicz, U., Burkowska, A., Walczak, M., 2014. Chitinolytic
- 625 microorganisms and their possible application in environmental protection. Current microbiology
- 626 68, 71-81.
- 627 Chelius, M., Triplett, E.J.M.e., 2001. The Diversity of Archaea and Bacteria in Association with
- the Roots of Zea mays L. 41.
- 629 Chen, L., Liu, L., Qin, S., Yang, G., Fang, K., Zhu, B., Kuzyakov, Y., Chen, P., Xu, Y., Yang,
- Y., 2019. Regulation of priming effect by soil organic matter stability over a broad geographic
- scale. Nature communications 10, 1-10.
- 632 Compant, S., Clément, C., Sessitsch, A., 2010. Plant growth-promoting bacteria in the rhizo-and
- endosphere of plants: their role, colonization, mechanisms involved and prospects for utilization.
- Soil Biology and Biochemistry 42, 669-678.
- Debnath, A., Mizuno, T., Miyoshi, S.-i., 2020. Regulation of chitin-dependent growth and
- natural competence in Vibrio parahaemolyticus. Microorganisms 8, 1303.
- Egamberdieva, D., Renella, G., Wirth, S., Islam, R., 2010. Enzyme activities in the rhizosphere
- of plants, Soil enzymology. Springer, pp. 149-166.
- Elias, J.E., Gygi, S.P., 2007. Target-decoy search strategy for increased confidence in large-scale
- protein identifications by mass spectrometry. Nature Methods 4, 207-214.
- Fransen, B., de Kroon, H., Berendse, F., 1998. Root morphological plasticity and nutrient
- acquisition of perennial grass species from habitats of different nutrient availability. Oecologia
- 643 115, 351-358.
- 644 Génard, M., Baldazzi, V., Gibon, Y., 2014. Metabolic studies in plant organs: don't forget
- dilution by growth. Frontiers in plant science 5, 85.
- Gobran, G., Clegg, S., Courchesne, F., 1998. Rhizospheric processes influencing the
- biogeochemistry of forest ecosystems, Plant-induced soil changes: Processes and feedbacks.
- 648 Springer, pp. 107-120.
- Hanzlíková, A., Šotolová, I., Jandera, A., 1989. Chitinase in the rhizosphere and on plant roots,
- Developments in soil science. Elsevier, pp. 293-299.
- Heitkötter, J., Marschner, B., 2018. Soil zymography as a powerful tool for exploring hotspots
- and substrate limitation in undisturbed subsoil. Soil Biology and Biochemistry 124, 210-217.
- Hodge, A., 2004. The plastic plant: root responses to heterogeneous supplies of nutrients. New
- 654 Phytologist 162, 9-24.
- Hunter, J.D., 2007. Matplotlib: A 2D graphics environment. Computing in science & engineering
- 656 9, 90-95.
- 657 Ilhardt, P.D., Nuñez, J.R., Denis, E.H., Rosnow, J.J., Krogstad, E.J., Renslow, R.S., Moran, J.J.,
- 658 2019. High-resolution elemental mapping of the root-rhizosphere-soil continuum using laser-
- induced breakdown spectroscopy (LIBS). Soil Biology and Biochemistry 131, 119-132.
- Kamiya, M., Urano, Y., Ebata, N., Yamamoto, M., Kosuge, J., Nagano, T., 2005. Extension of
- the Applicable Range of Fluorescein: A Fluorescein-Based Probe for Western Blot Analysis.
- Angewandte Chemie International Edition 44, 5439-5441.

- Kim, S., Pevzner, P.A., 2014. MS-GF+ makes progress towards a universal database search tool
- 664 for proteomics. Nature Communications 5.
- Kirk, J.L., Beaudette, L.A., Hart, M., Moutoglis, P., Klironomos, J.N., Lee, H., Trevors,
- J.T.J.J.o.m.m., 2004. Methods of studying soil microbial diversity. 58, 169-188.
- Kuzyakov, Y., Razavi, B.S., 2019. Rhizosphere size and shape: temporal dynamics and spatial
- stationarity. Soil Biology and Biochemistry 135, 343-360.
- 669 Li, K., Xing, R., Liu, S., Li, P., 2020. Chitin and chitosan fragments responsible for plant elicitor
- and growth stimulator. Journal of Agricultural and Food Chemistry 68, 12203-12211.
- Lin, V.S., Rosnow, J.J., McGrady, M.Y., Smercina, D.N., Nuñez, J.R., Renslow, R.S., Moran,
- J.J., 2020. Non-destructive spatial analysis of phosphatase activity and total protein distribution
- in the rhizosphere using a root blotting method. Soil Biology and Biochemistry 146, 107820.
- Liu, S., Razavi, B.S., Su, X., Maharjan, M., Zarebanadkouki, M., Blagodatskaya, E., Kuzyakov,
- Y., 2017. Spatio-temporal patterns of enzyme activities after manure application reflect
- mechanisms of niche differentiation between plants and microorganisms. Soil Biology and
- 677 Biochemistry 112, 100-109.
- Lovell, J.T., MacQueen, A.H., Mamidi, S., Bonnette, J., Jenkins, J., Napier, J.D., Sreedasyam,
- A., Healey, A., Session, A., Shu, S., 2021. Genomic mechanisms of climate adaptation in
- polyploid bioenergy switchgrass. Nature 590, 438-444.
- Ma, X., Liu, Y., Shen, W., Kuzyakov, Y., 2021. Phosphatase activity and acidification in lupine
- and maize rhizosphere depend on phosphorus availability and root properties: coupling
- zymography with planar optodes. Applied Soil Ecology 167, 104029.
- Ma, X., Liu, Y., Zarebanadkouki, M., Razavi, B.S., Blagodatskaya, E., Kuzyakov, Y., 2018a.
- Spatiotemporal patterns of enzyme activities in the rhizosphere: effects of plant growth and root
- 686 morphology. Biology and Fertility of Soils 54, 819-828.
- Ma, X., Zarebanadkouki, M., Kuzyakov, Y., Blagodatskaya, E., Pausch, J., Razavi, B.S., 2018b.
- Spatial patterns of enzyme activities in the rhizosphere: effects of root hairs and root radius. Soil
- Biology and Biochemistry 118, 69-78.
- Mendes, R., Garbeva, P., Raaijmakers, J.M., 2013. The rhizosphere microbiome: significance of
- plant beneficial, plant pathogenic, and human pathogenic microorganisms. FEMS microbiology
- 692 reviews 37, 634-663.
- Moran, J., McGrath, C., 2021. Comparison of methods for mapping rhizosphere processes in the
- context of their surrounding root and soil environments. BioTechniques 71, 604-614.
- Nakayasu, E.S., Nicora, C.D., Sims, A.C., Burnum-Johnson, K.E., Kim, Y.-M., Kyle, J.E.,
- Matzke, M.M., Shukla, A.K., Chu, R.K., Schepmoes, A.A., 2016. MPLEx: a robust and
- universal protocol for single-sample integrative proteomic, metabolomic, and lipidomic analyses.
- 698 MSystems 1, e00043-00016.
- Neiendam Nielsen, M., Sørensen, J., 1999. Chitinolytic activity of Pseudomonas fluorescens
- isolates from barley and sugar beet rhizosphere. FEMS Microbiology Ecology 30, 217-227.
- Nisa, R.M., Irni, M., Amaryllis, A., Sugeng, S., Iman, R., 2010. Chitinolytic bacteria isolated
- from chili rhizosphere: chitinase characterization and its application as biocontrol for whitefly
- 703 (Bemisia tabaci Genn.). American Journal of Agricultural and Biological Sciences 5, 430-435.
- Nuccio, E.E., Starr, E., Karaoz, U., Brodie, E.L., Zhou, J., Tringe, S.G., Malmstrom, R.R.,
- Woyke, T., Banfield, J.F., Firestone, M.K., 2020. Niche differentiation is spatially and
- temporally regulated in the rhizosphere. The ISME journal 14, 999-1014.
- Olander, L.P., Vitousek, P.M., 2000. Regulation of soil phosphatase and chitinase activityby N
- and P availability. Biogeochemistry 49, 175-191.

- Pathan, S.I., Ceccherini, M.T., Sunseri, F., Lupini, A., 2020. Rhizosphere as hotspot for plant-
- soil-microbe interaction, Carbon and Nitrogen Cycling in Soil. Springer, pp. 17-43.
- Razavi, B.S., Hoang, D.T., Blagodatskaya, E., Kuzyakov, Y., 2017. Mapping the footprint of
- nematodes in the rhizosphere: Cluster root formation and spatial distribution of enzyme
- activities. Soil Biology and Biochemistry 115, 213-220.
- Razavi, B.S., Zhang, X., Bilyera, N., Guber, A., Zarebanadkouki, M., 2019. Soil zymography:
- Simple and reliable? Review of current knowledge and optimization of the method. Rhizosphere
- 716 11, 100161.
- Reback, J., McKinney, W., Van den Bossche, J., 2020. Jbrockmendel. McKinney, W.
- Robertson, G.P., Hamilton, S.K., 2015. Long-Term Ecological Research at the Kellogg
- 719 Biological Station LTER site, In: Hamilton, S.K., Doll, J.E., Robertson, G.P. (Eds.), The
- 720 Ecology of Agricultural Lanscapes: Long-Term Research on the Path to Sustainability. Oxford
- 721 University Press, New York, pp. 1-32.
- Robertson, G.P., Klingensmith, K.M., Klug, M.J., Paul, E.A., Crum, J.R., Ellis, B.G., 1997. Soil
- resources, microbial activity, and primary production across an agricultural ecosystem.
- 724 Ecological Applications 7, 158-170.
- Sharma, N., Sharma, K., Gaur, R., Gupta, V., 2011. Role of chitinase in plant defense. Asian
- Journal of Biochemistry 6, 29-37.
- Slysz, G.W., Steinke, L., Ward, D.M., Klatt, C.G., Clauss, T.R., Purvine, S.O., Payne, S.H.,
- Anderson, G.A., Smith, R.D., Lipton, M.S., 2014. Automated data extraction from in situ
- protein-stable isotope probing studies. Journal of proteome research 13, 1200-1210.
- Spohn, M., 2014. Soil zymography–A novel technique for mapping enzyme activity in the
- rhizosphere, EGU General Assembly Conference Abstracts, p. 11870.
- Spohn, M., Carminati, A., Kuzyakov, Y., 2013. Soil zymography-a novel in situ method for
- mapping distribution of enzyme activity in soil. Soil Biology and Biochemistry 58, 275-280.
- Spohn, M., Kuzyakov, Y., 2014. Spatial and temporal dynamics of hotspots of enzyme activity
- in soil as affected by living and dead roots—a soil zymography analysis. Plant and Soil 379, 67-
- 736 77.
- 737 Steinke, L., Slysz, G.W., Lipton, M.S., Klatt, C., Moran, J.J., Romine, M.F., Wood, J.M.,
- Anderson, G., Bryant, D.A., Ward, D.M., 2020. Short-term stable isotope probing of proteins
- reveals taxa incorporating inorganic carbon in a hot spring microbial mat. Applied and
- environmental microbiology 86, e01829-01819.
- 741 Torsvik, V., Øvreås, L.J.C.o.i.m., 2002. Microbial diversity and function in soil: from genes to
- 742 ecosystems. 5, 240-245.
- Van Der Walt, S., Colbert, S.C., Varoquaux, G., 2011. The NumPy array: a structure for efficient
- numerical computation. Computing in science & engineering 13, 22-30.
- Veliz, E.A., Martínez-Hidalgo, P., Hirsch, A.M., 2017. Chitinase-producing bacteria and their
- role in biocontrol. AIMS microbiology 3, 689.
- Virtanen, P., Gommers, R., Oliphant, T.E., Haberland, M., Reddy, T., Cournapeau, D., Burovski,
- E., Peterson, P., Weckesser, W., Bright, J., 2020. SciPy 1.0: fundamental algorithms for
- scientific computing in Python. Nature methods 17, 261-272.
- Waskom, M., Botvinnik, O., O'Kane, D., Hobson, P., Ostblom, J., Lukauskas, S., Gemperline,
- 751 D.C., Augspurger, T., Halchenko, Y., Cole, J.B., 2018. mwaskom/seaborn: v0. 9.0 (July 2018).
- 752 DOI: https://doi.org/10.5281/zenodo1313201.

- Wei, S., Jacquiod, S., Philippot, L., Blouin, M., Sørensen, S.J., 2021. Spatial analysis of the root
- 754 system coupled to microbial community inoculation shed light on rhizosphere bacterial
- community assembly. Biology and Fertility of Soils 57, 973-989.
- Whipps, J.M., 2001. Microbial interactions and biocontrol in the rhizosphere. Journal of
- 757 experimental Botany 52, 487-511.
- White, R.A., Rosnow, J., Piehowski, P.D., Brislawn, C.J., Moran, J.J., 2021. In Situ Non-
- 759 Destructive Temporal Measurements of the Rhizosphere Microbiome 'Hot-Spots' Using
- 760 Metaproteomics. Agronomy 11, 2248.
- Winkler, A.J., Dominguez-Nuñez, J.A., Aranaz, I., Poza-Carrión, C., Ramonell, K., Somerville,
- S., Berrocal-Lobo, M., 2017. Short-chain chitin oligomers: Promoters of plant growth. Marine
- 763 drugs 15, 40.
- Zegeye, E.K., Sadler, N.C., Lomas, G.X., Attah, I.K., Jansson, J.K., Hofmockel, K.S., Anderton,
- 765 C.R., Wright, A.T., 2021. Activity-Based Protein Profiling of Chitin Catabolism. ChemBioChem
- 766 22, 717-723.

- 767 Zhang, X., Li, K., Xing, R., Liu, S., Chen, X., Yang, H., Li, P., 2018. miRNA and mRNA
- expression profiles reveal insight into chitosan-mediated regulation of plant growth. Journal of
- Agricultural and Food Chemistry 66, 3810-3822.